

Development of a 7-miRNA prognostic signature for patients with bladder cancer

Yingjie Xv^{1,*,#}, Ming Qiu^{2,*,#}, Zhaojun Liu³, Mingzhao Xiao^{1,*}, Fen Wang^{4,*}

¹Department of Urology, The First Affiliated Hospital of Chongqing Medical University, Chongqing, Yuzhong 400016, China

²Department of Urology, The People's Hospital of Dazu, Chongqing, Dazu 402360, China

³Department of Cardiology, The First Affiliated Hospital of Chongqing Medical University, Chongqing, Yuzhong 400016, China

⁴Department of Pathology, The People's Hospital of Dazu, Chongqing, Dazu 402360, China

*Equal contribution

#Co-first authors

Correspondence to: Mingzhao Xiao, Fen Wang; email: mingzhaoxiao@hospital.cqmu.edu.cn; 25240805@qq.com, <https://orcid.org/0000-0002-9939-9503>

Keywords: bladder cancer, miRNAs, prognostic signature, risk score, nomogram

Received: August 20, 2021

Accepted: February 12, 2022

Published: December 21, 2022

Copyright: © 2022 Xv et al. This is an open access article distributed under the terms of the [Creative Commons Attribution License](https://creativecommons.org/licenses/by/3.0/) (CC BY 3.0), which permits unrestricted use, distribution, and reproduction in any medium, provided the original author and source are credited.

ABSTRACT

Background: Bladder carcinoma (BC) represents one of the most prevalent malignant cancers, while predicting its clinical outcomes using traditional indicators is difficult. This study aimed to develop a miRNA signature for the prognostic prediction of patients with BC.

Materials and Methods: MiRNAs that expressed differentially were identified between 413 BC and 19 non-tumor patients, whose prognostic values were evaluated using univariate and multivariate Cox regression analyses. The independent prognostic factors were screened out and were used to establish a signature. The risk score of the signature was calculated. Receiver operating characteristic (ROC) curves and Kaplan-Meier curves were used to verify the predictive performance of the miRNA signature and the risk score. A nomogram was constructed which integrated with the miRNA signature and clinical parameters. Experiments were performed.

Results: 7 prognosis related miRNAs were selected as independent risk factors, and a 7-miRNA signature was constructed, with an area under ROC (AUC) of 0.721. The 7-miRNA-signature based risk score acts as an independent prognostic factor, with satisfactory predictive performance (AUC = 0.744). Increased miR-337-3p expressions were detected in tumor samples and BC cell lines than in non-tumorigenic tissues and cell lines. Experiments suggested that miR-337-3p induces the proliferation, migration, and invasion of BC cells.

Conclusion: The constructed 7-miRNA signature is a promising biomarker for predicting the prognosis of patients with BC, and miR-337-3p may act as a candidate therapeutic target in BC treatments.

INTRODUCTION

Bladder cancer (BC) is the ninth most common cancer worldwide, generating 165,000 deaths annually [1, 2]. There are two clinical subtypes of BC: non-muscle-invasive bladder cancer (NMIBC) and muscle-invasive bladder cancer (MIBC), in which NMIBC accounts for

approximately 75% of newly diagnosed bladder cancer patients. Most BC patients have long-term survival after undergoing the transurethral resection of the bladder tumor (TURBT). However, 10–15% of NMIBC patients may progress to MIBC, for which the 5-year overall survival (OS) is often less than 50% [3, 4]. Tumor-node-metastasis (TNM) classification and pathological

grade are used in clinical settings to predict patient prognosis. However, the predictive ability for individual clinical outcomes remains inadequate since these classification systems are indicators at a population level [5]. Therefore, novel prognostic biomarkers that reveal the mechanisms underlying tumorigenesis for personalized prognosis prediction and the development of effective treatment strategies are urgently needed.

MicroRNA (miRNA), a member of the small non-coding RNA family, is 21–23 nucleotides long that can interact with the 3' non-coding region of the target mRNA and regulate translation of corresponding proteins [6, 7]. Recent evidence indicates that miRNA regulates various steps in carcinogenesis, including cancer initiation, progression, metastasis, and patient survival [8, 9]. Various researches have proved that miRNAs could act as prognostic markers in various cancers, through microarray or RNA-sequencing technologies [10, 11]. Several miRNA signatures have been established to determine the prognosis of BC patients beyond their clinicopathological features, with satisfactory predictive performance [12–14]. However, only a few *in vitro* experiments have been conducted to confirm the correlation between discovered prognostic miRNAs and tumorigenesis.

In this study, differentially expressed miRNAs between BC and non-tumor tissues were mined via The Cancer Genome Atlas (TCGA) database, and a novel 7-miRNA based signature was established based on the prognosis relative miRNAs. Quantitative reverse transcription-based polymerase chain reaction (RT-qPCR) was used to detect the differentiated miRNAs' expressions in BC cell lines and clinical samples, followed by *in vitro* functional analysis. The 7-miRNA signature established in our study proved to be a novel biomarker for predicting the progression and OS in BC patients.

MATERIALS AND METHODS

Data collection and screening of differentially expressed miRNAs

The miRNA expression profiles and corresponding clinical data (age, sex, grade, and TNM classification) of 413 BC patients and 19 non-tumor patients were obtained from TCGA [15]. Patients with incomplete data or ambiguous overall survival were excluded. The “limma” package of the R language (version 4.0.2) was used to screen out the differentially expressed miRNAs (p values < 0.05 and $|\text{Log}_2\text{FC}|$ values >1), which were retained for further analysis [16].

Construction of miRNA prognostic signature

The mined differentially expressed miRNAs were subjected to univariate Cox regression analysis to

explore whether there were associations between them and patients' OS, and statistically significant miRNAs (p value < 0.001) were processed by multivariable Cox regression analysis. MiRNAs with statistically significance (p values < 0.05) in the multivariable Cox regression analysis were regarded as independent prognostic indicators for patients' survival and were utilized to construct a 7-miRNA signature.

The miRNAs' risk scores of each patient were calculated on the basis of the miRNAs' coefficients, and the median risk score acted as a boundary to categorize low- and high-risk BC patients. The differences between OS of the high- and low-risk groups were compared via Kaplan-Meier survival curve analysis and survival curves. The predictive ability of the 7-miRNA signature was assessed using the receiver operating characteristic (ROC) curve analysis generated by R packages “ggplot2” and “survivalROC.” The univariate and multivariate Cox regression analyses were used to evaluate the signature's independent predictive value in BC patients' survival.

Establishment and evaluation of the nomogram

A nomogram was established to predict the 1, 3, and 5-year OS in BC patients, through integration with the clinicopathological characteristics and risk score, using the “rms” package of the R (version 4.0.1). The clinical significance and concordance between the predicted and observed patients were evaluated via plotted time-dependent ROC curves.

Prediction of target genes and function enrichment analysis

Online analysis tools, miRDB (<http://www.mirdb.org/miRDB/index.html>), miRTarBase, and TargetScan (<http://www.targetscan.org/>), were employed to predict the mRNAs that are downstream targets of our signature miRNAs. Owing to the large number of genes mined along with the three algorithms that determined different target binding, the ‘Draw Venn Diagram’ (<http://bioinformatics.psb.ugent.be/webtools/Venn/>) tool was used to screen the overlapping mRNAs, which were subsequently analyzed via the “enrichplot” package in the R language to annotate GO and enrich the KEGG pathway. The protein-protein interaction (PPI) network analysis of the target genes was conducted via the String Database.

Clinical sample collection

The clinical samples, including 13 BC tissues and their paired non-tumor tissues, were obtained from histopathologically diagnosed BC patients who underwent curative resection at the First Affiliated Hospital of Chongqing Medical University between May 2020 and May 2021. Prior to conducting the study, the

Table 1. MiRNA and oligonucleotide sequences.

miRNA	Primer sequence (5' to 3')
miR-151a-5p	GCAGGTCGAGGAGCTCACAG
miR-216a-5p	GCAGGTAATCTCAGCTGGCAA
miR-337-3p	GCGTGCTCCTATATGATGCCT
U6	ATGGACTATCATATGCTTACCGAT
miR-337-3p-mimics-F	CUCCUAUAUGAUGCCUUUCUUC
miR-337-3p-mimics-R	AGAAAGGCAUCAUAUAGGAGUU
miR-337-3p-inhibitor	GAAGAAAGGCAUCAUAUAGGAG

institutional Review Board of the First Affiliated Hospital of Chongqing Medical University approved the study protocols, and the requirement for patients' informed consent was waived.

Cell culture

The BC cell lines (T24, 5637, UMUC3, TCCSUP, and RT4) and a non-tumorigenic bladder cell line (SV-HUC-1) were purchased from the American Type Culture Collection (ATCC, Manassas, VA, USA). Cell cultures were conducted under 37°C in a humidified incubator supplemented with 5% CO₂. The Dulbecco's Modified Eagle Medium (DMEM; Invitrogen, Carlsbad, CA, USA) was used to culture UMUC3, RT4, and SV-HUC-1 cells, while the Roswell Park Memorial Institute (RPMI) 1640 Medium was used to culture the T24, 5637, and TCCSUP cells. Ten percent fetal bovine serum (FBS; Invitrogen, Carlsbad, CA, USA) and 1% penicillin-streptomycin were added to the medium.

RNA isolation and RT-qPCR

The TRIzol reagent (Invitrogen, Thermo Fisher Scientific, Waltham, MA, USA) was used to extract total RNA from BC tissues and above cells, based on the manufacturer's protocol. One microgram of total RNA, in addition to the PrimeScript RT reagent kit (Takara Bio, Kusatsu, Japan), were utilized to synthesize the complementary DNA (cDNA). RT-qPCR was performed using the SYBR-Green assay (Takara Bio, Kusatsu, Japan) on an ABI 7500 Real-Time PCR system (Applied Biosystems, Waltham, MA, USA).

The U6 snRNA (ID 001973, Thermo Fisher Scientific, Waltham, MA, USA) was used as an internal reference, and the relative miRNA expression was calculated using the 2^{-ΔΔCq} method [17]. The primer sequences (Invitrogen, Thermo Fisher Scientific, Waltham, MA, USA) are listed in Table 1.

Oligonucleotide transfection

The miRNA mimics, miRNA inhibitor, and negative control (NC) were purchased from Tsingke

Biotechnology (Beijing, China). The Lipofectamine 3000 (Invitrogen, Thermo Fisher Scientific, Waltham, MA, USA) was employed to conduct oligonucleotide transfection. UMUC3 and 5637 cells were first seeded in 6-well plates, separately, and grown until they reached 80% confluence. Next, a mixture containing miRNA mimics, NC, miRNA inhibitor, and Lipofectamine 3000 reagent were added to the cells. The sequences of the mimics and inhibitor are listed in Table 1.

Cell invasion assay

At 48 h post-transfection, the UMUC3 and 5637 cells were harvested and resuspended in serum-free RPMI 1640 medium. After cell counting, 100 μL medium containing 5 × 10⁴ cells were added into the upper chamber of a transwell plate (Corning Incorporated, Corning, NY, USA) that were precoated with Matrigel, while 700 μL medium containing 10% FBS was added to the lower chamber. The cells were incubated for 24 hours under normal conditions. Cells that passed through the transwell membrane were fixed with 4% paraformaldehyde and stained with 0.5% crystal violet dye. The stained cells were imaged and counted under a microscope at ×200 magnification.

Wound healing assay

A total of 5 × 10³ 5637 and UMUC3 cells were seeded in the 6-well plates and were classified into NC, miRNA-inhibitor, and miRNA-mimics groups. 48 h after oligonucleotide transfection, the cells were cultured until they reached 100% confluence. A 200 μl sterile pipette tip was used to scratch the confluent monolayer. The phosphate-buffered-saline (PBS) was used to wash the wounded cell layers three times and the washed cells were incubated with serum-free medium for 48 h. The migration status of wounded cell layers was assessed by imaging the scratched region at 0 and 24 h (magnification ×100).

Cell proliferation assay

Cell proliferation was assessed via the Cell Counting Kit-8 (CCK-8, Dojindo Molecular Technologies,

Rockville, MD, USA) assay. 48 h after transfection, UMUC3 and 5637 cells were seeded (1×10^3 cells/well) into the 96-well plates. After 12, 24, 48, and 72 h of culture, 10 μ L of CCK-8 agent was added to each well and incubated for 1 h. The microplate reader (Infinite 200 PRO, TECAN, Männedorf, Switzerland) was used to measure the absorbance at 490 nm.

Statistical analysis

The GraphPad Prism software (version 8.0) and R software (version 4.0.2) were employed to process all statistical analyses, and statistical significance was set at $p < 0.05$.

Data availability statement

The original contributions presented in the study are included in the Article/Supplementary Material.

RESULTS

Identification of differentially expressed miRNAs

A total of 432 samples comprising, with complete clinicopathological data such as: age, sex, tumor grade, and TNM status, were included in our study. The

“limma” package of the R language was utilized to explore the differentially expressed miRNAs between BC samples and non-tumor samples. miRNAs with $|\log_2FC|$ of >1 and $P < 0.05$, were screened. The volcano plot identified 473 differentially expressed miRNAs (Supplementary Table 1), among which, expression of 379 miRNAs was upregulated and those of 94 miRNAs was downregulated (Figure 1A, Supplementary Table 1). The heatmap demonstrates unsupervised clustering of all the differentially expressed miRNAs (Figure 1B). Univariable Cox regression analysis between the differential expression miRNAs and survival data revealed 18 OS-associated miRNAs (Figure 1C). Multivariate Cox regression analysis filtered 7 miRNAs (miR-151a-5p, miR-216a-5p, miR-337-3p, let-7c-5p, miR-125b-2-3p, miR-590-3p, and miR-652-3p) that may predict prognosis of BC patients (Supplementary Table 2); four were negatively correlated while three were positively correlated to OS (Figure 2A–2G).

Establishment and evaluation of the predictive 7-miRNA signature

Prognostic miRNAs including: miR-151a-5p, miR-216a-5p, miR-337-3p, hsa-let-7c-5p, miR-125b-2-3p, miR-590-3p, and miR-652-3p were fed into the

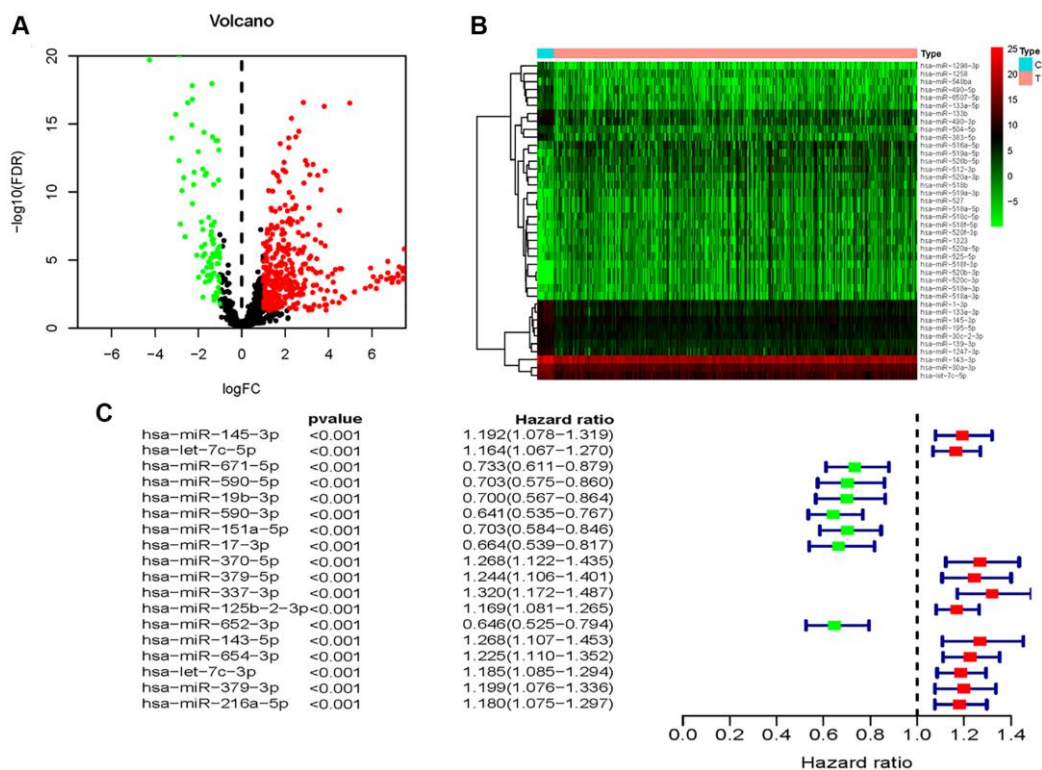


Figure 1. Identification of OS-related differentially expressed miRNAs between BC and non-tumor tissues. (A) Volcano plot of 437 identified differentially expressed miRNAs. **(B)** The heatmap of the unsupervised clustering of the differentially expressed miRNAs. **(C)** The univariate Cox regression analysis for exploration of miRNAs that were significantly correlated with OS of BC patients.

signature (namely 7-miRNA signature), based on the calculated risk score [risk score = $(-0.4762 \times \text{let-7c-5p expressions}) + (-0.3482 \times \text{miR-590-3p expressions}) + (-0.2106 \times \text{miR-151a-5p expressions}) + (0.1619 \times \text{miR-337-3p expressions}) + (0.3912 \times \text{miR-125b-2-3p expressions}) + (-0.2371 \times \text{miR-652-3p expressions}) + (0.1525 \times \text{miR-216a-5p expressions})$] for each patient. A median value of the risk score was set, and patients were divided into low- and high-risk groups based on this (Figure 3A).

The scatter dot plot indicated that patients in low-risk group presented a longer survival duration (Figure 3B). The expression patterns of these seven miRNAs in the 413 BC patients are displayed in Figure 3C, indicating that high-risk scores tend to express high-risk miRNAs, while low-risk scores were the opposite. Similarly, an increased mortality rate was observed in the high-risk group (Figure 3D). The 7-miRNA signature yielded a satisfactory predictive ability, with 1-, 3-, and 5-years AUC values of 0.682, 0.700, and 0.721, respectively (Figure 3E–3G).

Prognostic value of the 7-miRNA-signature based on risk score

The univariate and multivariate Cox analyses were conducted in order to explore the prognostic value of the 7-miRNA-signature based on risk score in BC patients. The risk score of the 7-miRNA signature along with clinicopathological characteristics such as age, sex, grade, stage, and TNM status were used as covariates. Covariates that were significantly associated with survival in univariate Cox analysis (age [$P < 0.001$],

stage [$P < 0.001$], T status [$P < 0.001$], N status [$P < 0.001$], M status [$P = 0.025$], and risk score [$P < 0.001$]) were subjected to multivariate Cox analysis. Results indicated that age (HR = 1.020, 95% CI: 1.003–1.038, $P = 0.021$) and risk score (HR = 1.720, 95% CI: 1.445–2.047, $P < 0.001$) are independent prognostic indicators (Figure 4A, 4B). Moreover, multi-parameter ROC curve analyses showed that the risk score achieved the most satisfactory predictive performance compared with clinicopathological characteristics, with an AUC value of 0.744, indicating that the 7-miRNA risk score is a promising prognostic biomarker (Figure 4C).

Next, we created a nomogram that integrating with the 7-miRNA-signature risk score and clinicopathological prognostic factors, which presented better predictive performance for 5-year OS (Figure 4D).

Target gene prediction and functional enrichment analysis

Overall, 387 overlapping mRNAs were identified via three online analysis tools (Figure 5). GO enrichment analysis indicated that these target genes were mainly enriched in 11 biological processes, 10 cellular components, and 6 molecular functions, among which cell morphogenesis involved in neuron differentiation, axon development, and axonogenesis; synaptic membrane, extracellular matrix, and postsynaptic membrane; and DNA-binding transcription repressor activity, RNA polymerase II-specific, glycosaminoglycan binding, and extracellular matrix structural constituent represented the top three biological processes, respectively (Figure 6A). Moreover, KEGG pathway

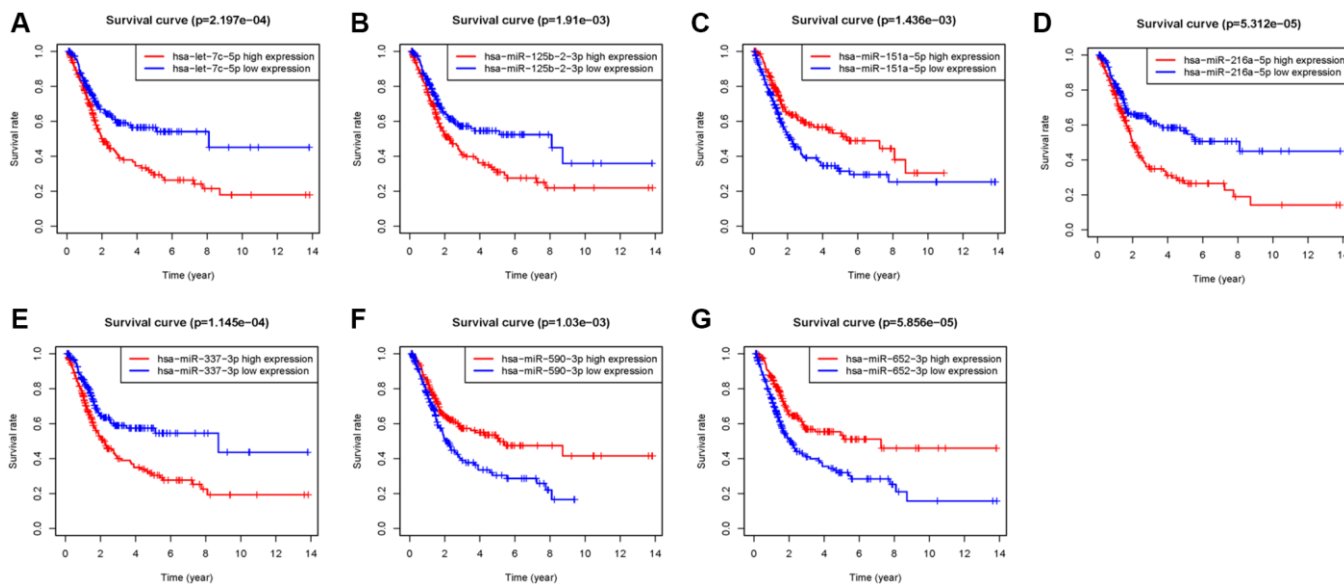


Figure 2. Kaplan–Meier survival analysis of 7 prognostic-related miRNAs. (A) let-7c-5p, (B) miR-125b-2-3p, (C) miR-151a-5p, (D) miR-216a-5p, (E) miR-337-3p, (F) miR-590-3p, (G) miR-652-3p.

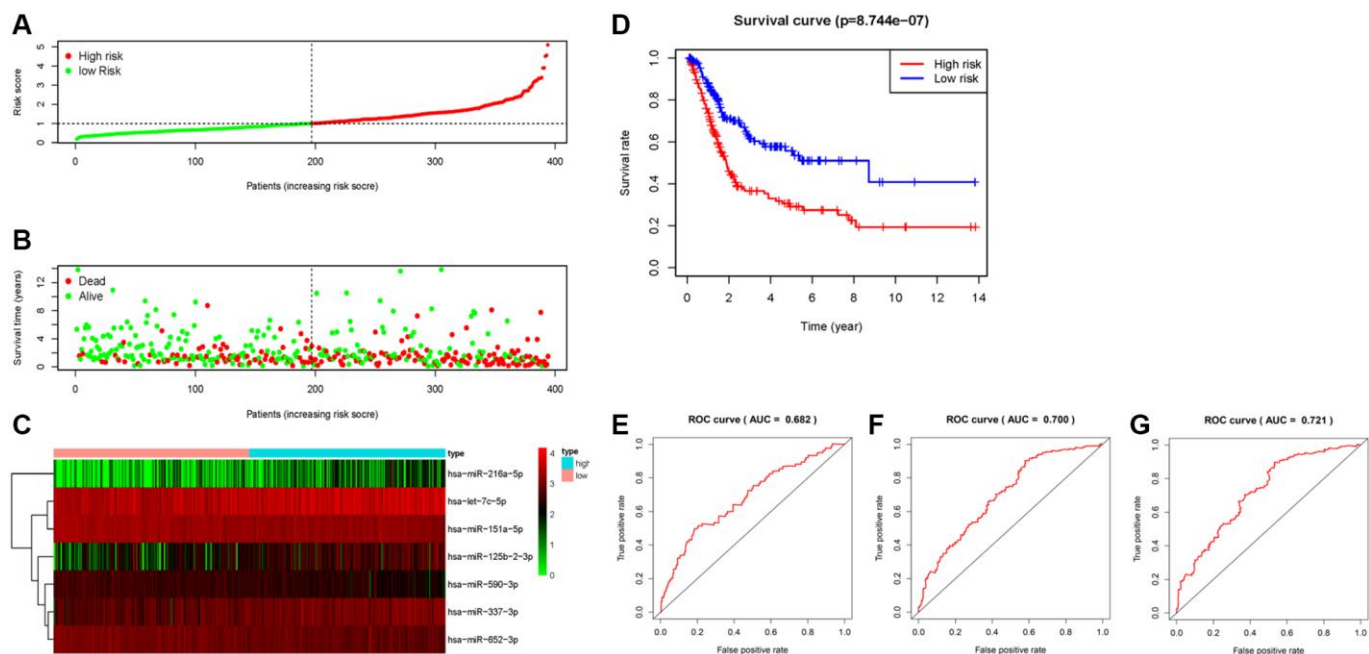


Figure 3. Construction and evaluation of the predictive 7- miRNA signature. (A) The distribution of the 7-miRNA risk score for each patient. (B) Scatter dot plot for survival rates of patients with BC in low- and high-risk groups. (C) Heatmap for the different expression of prognostic signature-related miRNAs in different risk groups. (D) Kaplan–Meier curve of OS in high- and low-risk groups. (E–G) ROC curves of the 7-miRNA signature for prediction of 1-, 3- and 5-year OS.

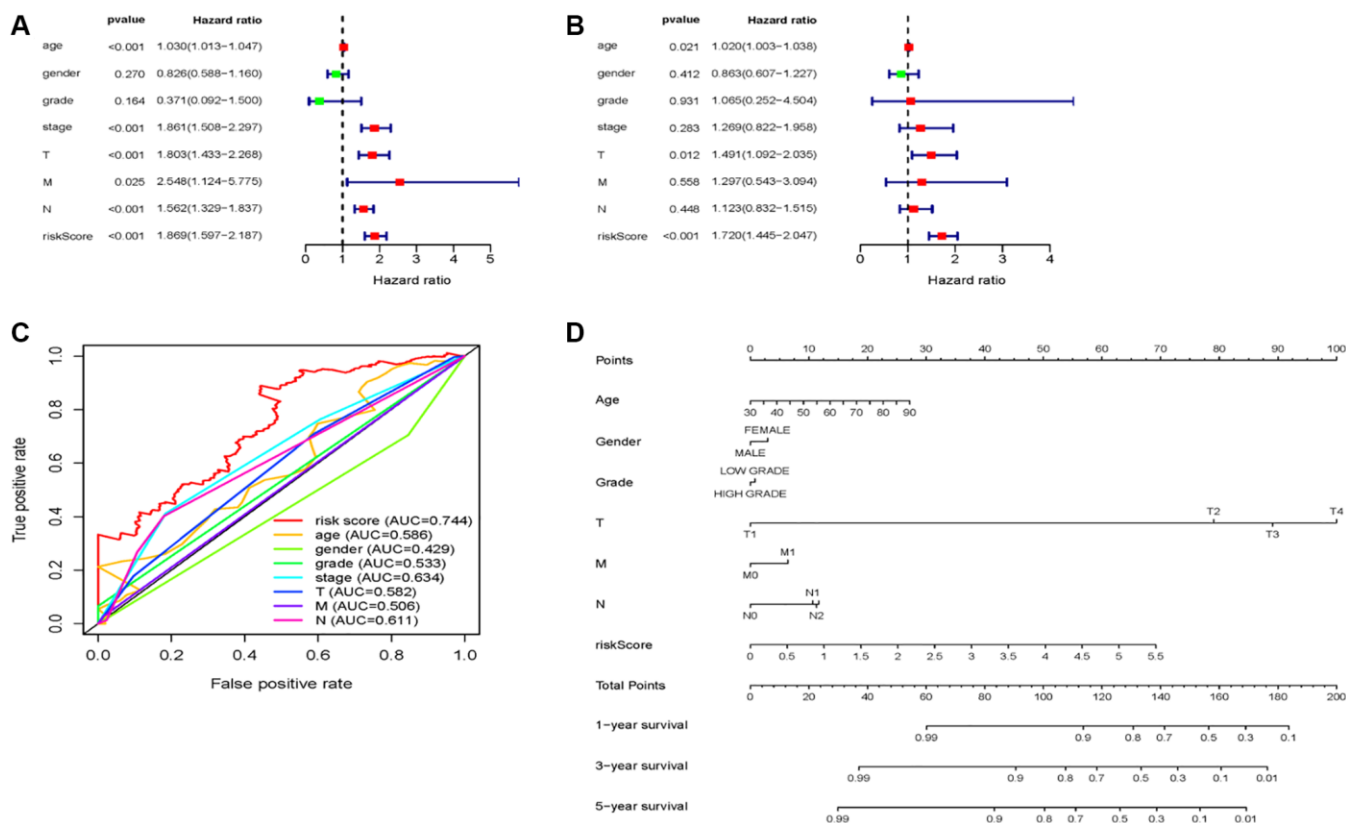


Figure 4. 7 miRNA-signature based risk score predicts OS in patients with BC. (A) Univariable and (B) multivariable analyses for the risk score and clinic-pathological features. (C) ROC curves of the 7 miRNA-signature based risk score and clinicopathological characteristics. (D) A nomogram integrates clinicopathological parameters and the risk score.

enrichment analysis was conducted, indicating the following seven pathways were enriched with the target genes: calcium signaling pathway, cAMP signaling pathway, axon guidance, circadian entrainment, renin secretion, regulation of lipolysis in adipocytes, and GnRH secretion (Figure 6B).

Detection of miR-337-3p, miR-216a-5p, and miR-151a-5p expression in clinical samples and cell lines

MiR-337-3p, miR-216a-5p, and miR-151a-5p expressions were measured in clinical samples and cell lines using RT-qPCR. As shown in Figure 7A–7C, in the BC

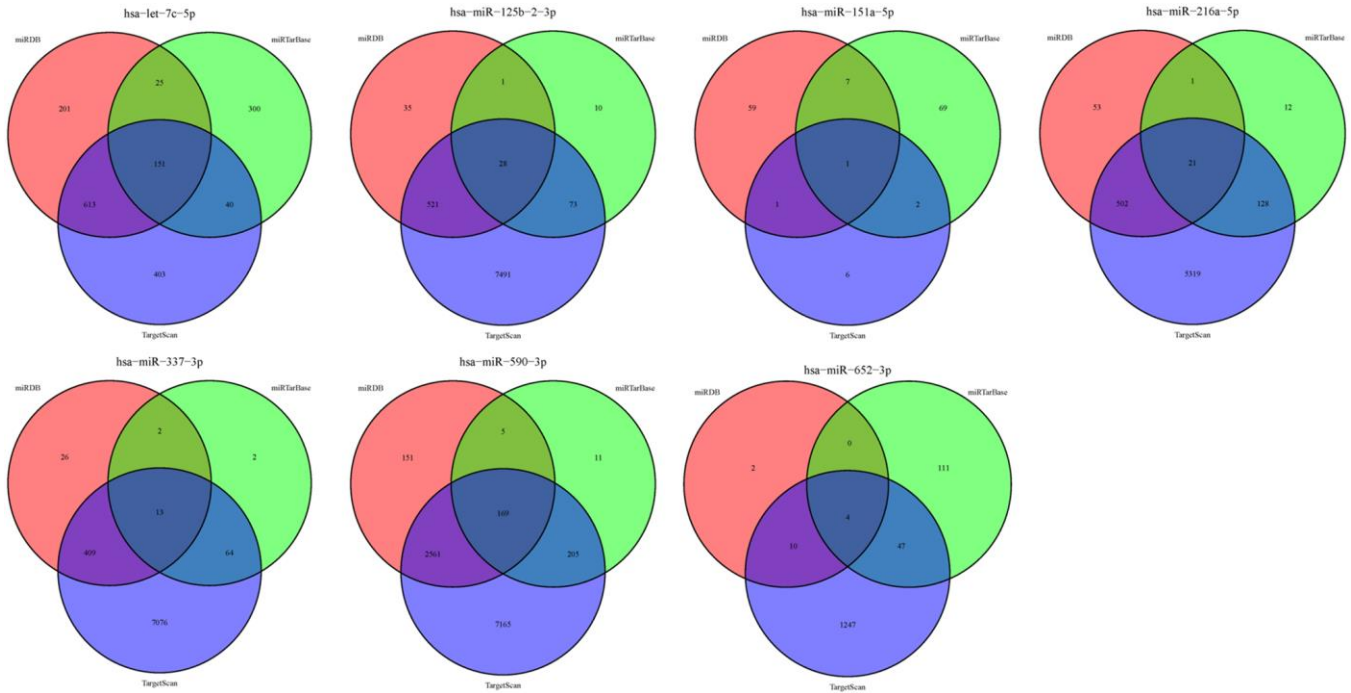


Figure 5. Target genes of the 7 miRNAs.

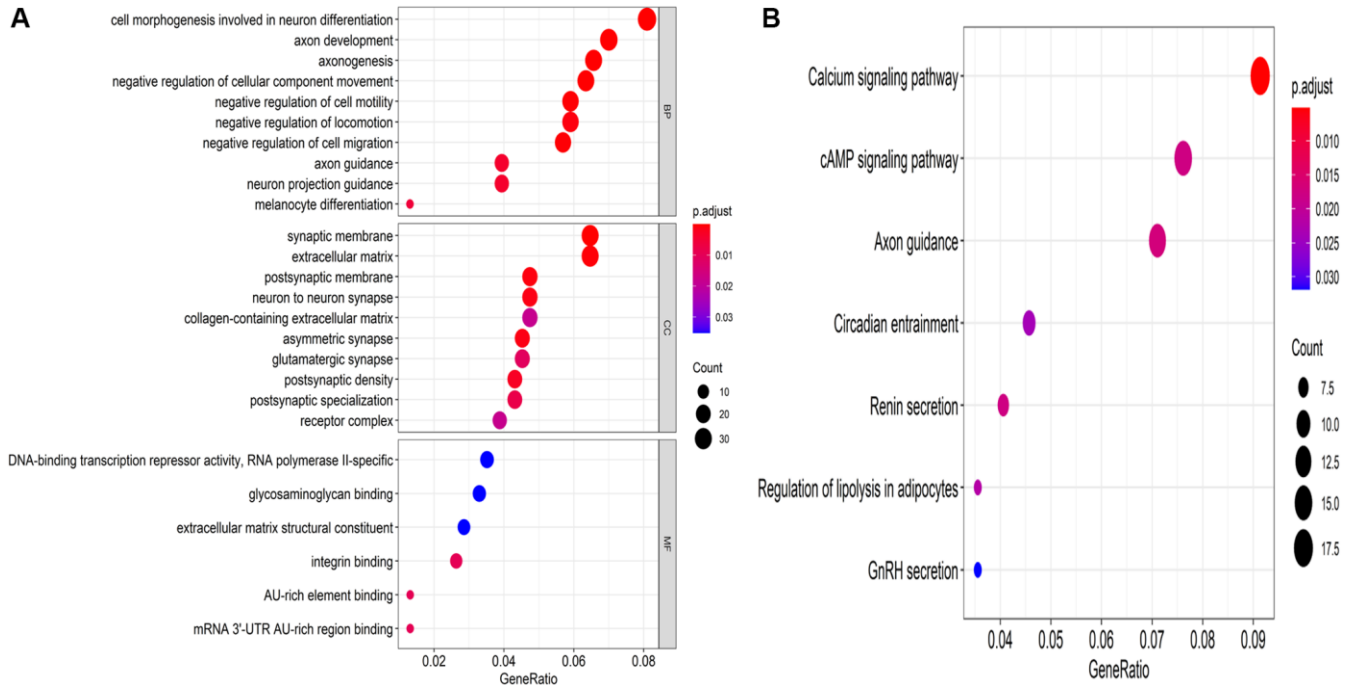


Figure 6. Underlying molecular functions of the target genes. (A) GO enrichment analysis and (B) KEGG pathway enrichment analysis of the target genes.

tissues, the expression levels of miR-337-3p and miR-216a-5p were significantly increased, while the miR-151a-5p expressions were markedly decreased, comparing with non-tumor tissues. Even miR-216a-5p and miR-151a-5p levels were inconsistent with the results obtained in paired clinical samples; miR-337-3p expression was still significantly upregulated in BC cell lines, indicating that miR-337-3p promotes tumorigenesis (Figure 7D–7F). Thus, owing to its consistently high expressions, we speculate that miR-337-3p promotes the development and progression of bladder cancer.

MiR-337-3p induces proliferation, migration, and invasion in BC cells

The miR-337-3p mimics, NC, and miR-337-3p inhibitor were transfected into UMUC3 and 5,637 cells. The corresponding upregulated or downregulated miR-337-3p expressions were detected (Figure 8A, 8B). The wound healing assay showed that miR-337-3p overexpression obviously increased the migration rate of UMUC3 and 5637 cells, while opposite results were observed in miR-337-3p inhibitor groups (Figure 8C, 8E). Transwell invasion assays revealed that the group overexpressing miR-337-3p showed increased cell invasion, while the groups transfected with miR-337-3p

inhibitor did not (Figure 8D, 8F). In addition, as demonstrated in Figure 8G–8J, the CCK-8 assay reduced cell proliferation in UMUC3- and 5637- cells transfected with miR337-3p inhibitor, while cells transfected with miR-337-3p mimics showed increased cell proliferation. In conclusion, overexpression of miR-337-3p enhances the proliferation, migration, and invasion abilities of BC cells.

DISCUSSION

Traditional predictive indicators, such as TNM staging and pathological grade, have a limited ability to predict BC prognosis. Considering the high mortality rate of patients with NMIBC, novel prognostic indicators that can more accurately predict patient prognosis are urgently needed. In the present study, seven BC prognosis-related miRNAs (miR-151a-5p, miR-216a-5p, miR-337-3p, hsa-let-7c-5p, miR-125b-2-3p, miR-590-3p, and miR-652-3p) were identified to establish a 7-miRNA signature, which obtained an AUC value of 0.721 in terms of predicting 5-year OS. The risk score of the 7-miRNA signature provided an increased predictive ability (AUC = 0.744). The expression levels of 3 miRNAs (miR-151a-5p, miR-216a-5p, and miR-337-3p) along with their potential molecular regulation in BC cells were investigated via experiments.

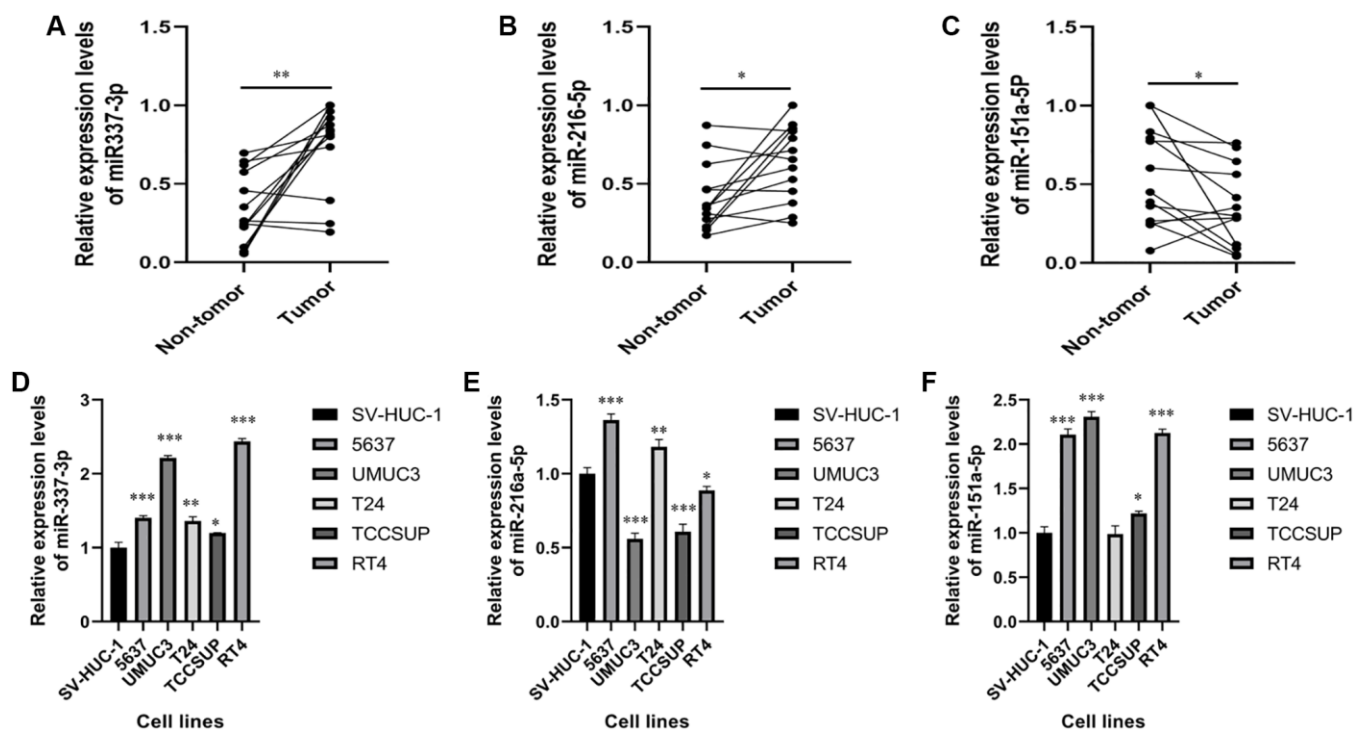


Figure 7. Expression levels of miR-337-3p, miR-216a-5p and miR-151a-5p expressions in clinical samples and cell lines. (A–C) RT-PCR shows that the expression levels of miR-337-3p, miR-216a-5p were significantly higher in BC tissues, while the expression levels of miR-151a-5p were lower in BC tissues, compared with non-tumor tissues. (D–F) The expression levels of miR-337-3p and miR-151a-5p were increased in the bladder cancer cell lines, while the expression levels of miR-216a-5p was decreased, compared with non-tumorigenic bladder cell line. * $p < 0.05$, ** $p < 0.01$, *** $p < 0.001$.

Several previous studies have reported the predictive value of miRNA signatures in patients with BC. Yin et al. [12] developed a 21-miRNA signature to predict the OS of BC patients, proving that bioinformatic-rooted miRNA-signatures can be used for predicting prognosis in BC patients. Using meta-analysis, Zhou et al. [18] screened eight miRNAs that correlate with the survival of patients with BC, and built an 8-miRNA signature with predictive and prognostic value. Their predictive miRNA-signatures achieved approximate AUCs of 0.7, but neither Yin et al. nor Zhou et al. validated their findings *in vivo* or *in vitro* experiments or revealed the underlying molecular mechanisms. In this study, 473 differentially expressed miRNAs were observed between 413 BC specimens and 19 non-tumor specimens using the “limma” package in R. The univariate and multivariate Cox regression analysis yielded seven novel prognosis-related miRNAs, which were employed to build a 7-miRNA signature. The signature-based risk score was calculated, which indicated that patients in the low-risk group had a longer OS compared with high-risk group. The

7-miRNA signature and risk score exhibited favorable predictive abilities, with AUC values of 0.721 and 0.744, respectively. In addition, to facilitate clinical application, we constructed a nomogram that incorporated risk scores and clinicopathological factors, showing a better prognostic value than a single parameter.

To further explore the molecular functions of these miRNAs, we attempted to validate their expressions in paired clinical samples and cell lines. A literature review of these seven miRNAs, using studies published on PubMed, revealed that these miRNAs are involved in the progression of bladder cancer or other cancers. Let-7c-5p is considered to be associated with the pathological grade of colon cancer, and may restrain lymph node metastasis in patients with breast cancer [19, 20]. Overexpression of miR-125b-2-3p may promote metastasis of clear cell renal cell cancer by targeting EGR1, leading to poor prognosis [21]; it also plays an important role in regulating the proliferation of colorectal cancer and oral squamous cell carcinoma by

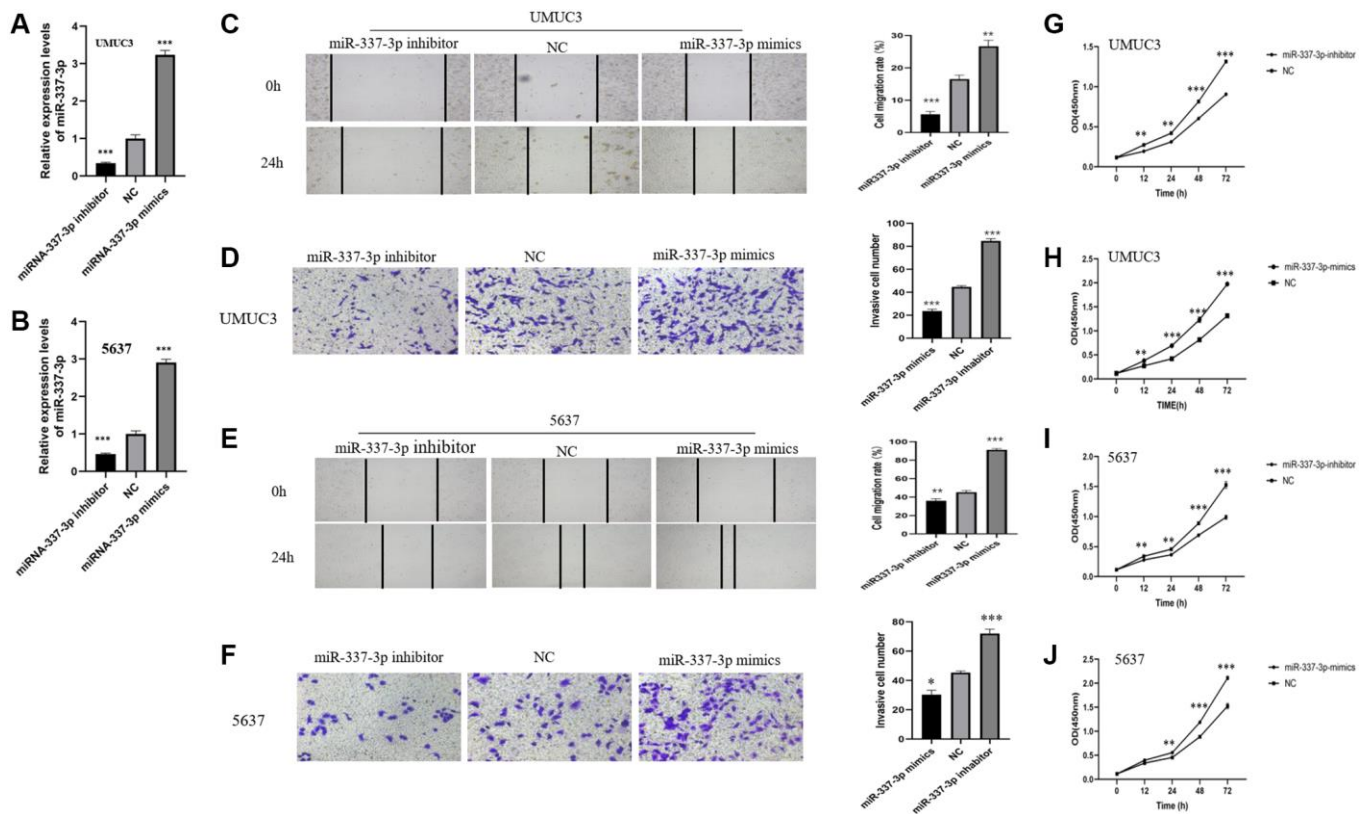


Figure 8. MiR-337-3p induces proliferation, migration, and invasion in BC cells. MiR-337-3p expressions in (A) UMUC3 and (B) 5637 cells were increased by the miR-337-3p mimics transfection and decreased by miR-337-3p inhibitor transfection, compared with the NC group. Wound healing assays (magnification, $\times 100$) and transwell invasion assays (magnification, $\times 200$) revealed that after transfection of miR-337-3p inhibitor, the cell migration rates and invasive cell number of UMUC3 cells (C, D) and 5637 cells (E, F) were restrained, while miR-337-3p mimics transfection promoted migration and invasion of UMUC3 (C, D) and 5637 (E, F) cells. CCK8 assays indicated that overexpression of miR-337-3p promoted proliferation activities of UMUC3 (G, H) and 5637 (I, J) cells, while miR-337-3p inhibitor groups acted the opposite. * $p < 0.05$, ** $p < 0.01$, *** $p < 0.001$.

acting as a downstream target of long noncoding RNAs, XIST and AC007271.3 [22, 23]. MiR-590-3p reportedly promotes nasopharyngeal and ovarian cancer carcinogenesis, and acts to inhibit invasion and metastasis in triple-negative breast cancer [24–26]. Ji et al. [27] demonstrated that miR-652-3p may be a serum indicator to predict tumor relapse and treatment outcomes in patients with colorectal cancer. In addition, hsa-let-7c-5p, miR-125b-2-3p, miR-590-3p, and miR-652-3p have been reported to regulate biological functions such as migration, proliferation, invasion, and apoptosis of BC [28–31]. Although miR-151a-5p is reportedly a prognostic factor for prostate cancer and lung adenocarcinoma [32, 33], miR-216a-5p acts as a suppressor in pancreatic cancer and breast cancer by targeting downstream mRNAs [34, 35]. Overexpression of miR-337-3p suppresses the migration and invasion of cervical cancer and ovarian cancer cells [36, 37]. These studies indicate that the miRNAs used to construct the 7-miRNA signature in our study may be clinically important cancer biomarkers involved in multiple signaling pathways in various tumors. However, to the best of our knowledge, miR-151a-5p, miR-216a-5p, and miR-337-3p have not been verified to predict prognosis or regulate molecular functions of BC. Therefore, we investigated the expression of miR-151a-5p, miR-216a-5p, and miR-337-3p in clinical samples and cell lines. RT-qPCR results show that compared with non-tumor tissues and non-tumorigenic bladder cell lines, miR-337-3p is overexpressed in tumor tissues and BC cell lines, while inconsistent results were observed in miR-151a-5p and miR-216a-5p expressions. Considering that patients with decreased miR-337-3p expression had a longer survival time (Figure 2), miR-337-3p was preliminarily identified to affect the biological progression of BC cells.

To better understand the molecular functions of these seven miRNAs, their target genes were identified using bioinformatic tools. We conducted GO enrichment and KEGG pathway enrichment analyses. GO terms showed that these target genes mainly affect biological functions, such as cell morphogenesis involved in neuron differentiation and axon development. KEGG pathway enrichment analysis revealed that these target genes are highly enhanced in the calcium signaling pathway, cAMP signaling pathway, axon guidance, and so on. Based on these results, we examined the molecular functions of miR-337-3p via wound healing, transwell invasion, and CCK8 assays, demonstrating that forced expression of miR-337-3p enhances the proliferation, migration, and invasion abilities of BC cells.

This study had several limitations. First, as a retrospective study, selection bias may have been inevitable. Second, we did not divide the dataset into

training and validation sets due to the insufficient sample size. Thus, large-scale prospective studies and additional *in vivo* and *in vitro* validation studies are warranted to confirm our findings and reveal the molecular mechanisms underlying the effects of miR-337-3p action in BC.

CONCLUSIONS

In this study, we present a novel 7-miRNA signature that may be a promising prognostic biomarker for patients with BC. This 7-miRNA signature can act as an independent prognostic indicator for BC. Integrating the 7-miRNA signature and other prognostic factors, we established a predictive model that showed a better prognostic value than a single parameter. We further explored the potential correlations between miR-151a-5p, miR-216a-5p, and miR-337-3p and the malignant biological behavior of BC cells, and found that miR-337-3p may not only be a novel prognostic biomarker for patients with BC, but also acts as a candidate therapeutic target in BC treatment.

AUTHOR CONTRIBUTIONS

Yingjie Xv and Mingzhao Xiao conceived the project. Yingjie Xv, Ming Qiu and Fen Wang analyzed the data and wrote the paper. Yingjie Xv and Zhaojun Liu conducted the experiments. Yingjie Xv and Ming Qiu are co-first authors; Mingzhao Xiao and Fen Wang are co-correspondence authors. All authors contributed to the article and approved the submitted version.

ACKNOWLEDGMENTS

The authors would like to acknowledge all clinicians and technicians of urology department in our institution that provided us professional advice and guidance.

CONFLICTS OF INTEREST

The authors declare that the research was conducted in the absence of any commercial or financial relationships that could be construed as potential conflicts of interest.

ETHICAL STATEMENT AND CONSENT

Prior to conducting the study, the institutional Review Board of the First Affiliated Hospital of Chongqing Medical University approved the study protocols, and the requirement for patients' informed consent was waived.

FUNDING

The project was funded by the Chongqing Municipal Health Committee (CQYC2020020318).

REFERENCES

1. Antoni S, Ferlay J, Soerjomataram I, Znaor A, Jemal A, Bray F. Bladder Cancer Incidence and Mortality: A Global Overview and Recent Trends. *Eur Urol*. 2017; 71:96–108.
<https://doi.org/10.1016/j.eururo.2016.06.010>
PMID:[27370177](https://pubmed.ncbi.nlm.nih.gov/27370177/)
2. Bellmunt J, Kim J, Reardon B, Perera-Bel J, Orsola A, Rodriguez-Vida A, Wankowicz SA, Bowden M, Barletta JA, Morote J, de Torres I, Juanpere N, Lloreta-Trull J, et al. Genomic Predictors of Good Outcome, Recurrence, or Progression in High-Grade T1 Non-Muscle-Invasive Bladder Cancer. *Cancer Res*. 2020; 80:4476–86.
<https://doi.org/10.1158/0008-5472.CAN-20-0977>
PMID:[32868381](https://pubmed.ncbi.nlm.nih.gov/32868381/)
3. Burger M, van der Aa MN, van Oers JM, Brinkmann A, van der Kwast TH, Steyerberg EC, Stoehr R, Kirkels WJ, Denzinger S, Wild PJ, Wieland WF, Hofstaedter F, Hartmann A, Zwarthoff EC. Prediction of progression of non-muscle-invasive bladder cancer by WHO 1973 and 2004 grading and by FGFR3 mutation status: a prospective study. *Eur Urol*. 2008; 54:835–43.
<https://doi.org/10.1016/j.eururo.2007.12.026>
PMID:[18166262](https://pubmed.ncbi.nlm.nih.gov/18166262/)
4. Lamm D, Persad R, Brausi M, Buckley R, Witjes JA, Palou J, Böhle A, Kamat AM, Colombel M, Soloway M. Defining progression in nonmuscle invasive bladder cancer: it is time for a new, standard definition. *J Urol*. 2014; 191:20–7.
<https://doi.org/10.1016/j.juro.2013.07.102>
PMID:[23973937](https://pubmed.ncbi.nlm.nih.gov/23973937/)
5. Solomon JP, Hansel DE. Prognostic factors in urothelial carcinoma of the bladder: histologic and molecular correlates. *Adv Anat Pathol*. 2015; 22:102–12.
<https://doi.org/10.1097/PAP.0000000000000050>
PMID:[25664945](https://pubmed.ncbi.nlm.nih.gov/25664945/)
6. Stefani G, Slack FJ. Small non-coding RNAs in animal development. *Nat Rev Mol Cell Biol*. 2008; 9:219–30.
<https://doi.org/10.1038/nrm2347>
PMID:[18270516](https://pubmed.ncbi.nlm.nih.gov/18270516/)
7. Bartel DP. MicroRNAs: target recognition and regulatory functions. *Cell*. 2009; 136:215–33.
<https://doi.org/10.1016/j.cell.2009.01.002>
PMID:[19167326](https://pubmed.ncbi.nlm.nih.gov/19167326/)
8. Sawaki K, Kanda M, Kodera Y. Review of recent efforts to discover biomarkers for early detection, monitoring, prognosis, and prediction of treatment responses of patients with gastric cancer. *Expert Rev Gastroenterol Hepatol*. 2018; 12:657–70.
<https://doi.org/10.1080/17474124.2018.1489233>
PMID:[29902383](https://pubmed.ncbi.nlm.nih.gov/29902383/)
9. Hayes J, Peruzzi PP, Lawler S. MicroRNAs in cancer: biomarkers, functions and therapy. *Trends Mol Med*. 2014; 20:460–9.
<https://doi.org/10.1016/j.molmed.2014.06.005>
PMID:[25027972](https://pubmed.ncbi.nlm.nih.gov/25027972/)
10. Luo Y, Chen L, Wang G, Xiao Y, Ju L, Wang X. Identification of a three-miRNA signature as a novel potential prognostic biomarker in patients with clear cell renal cell carcinoma. *J Cell Biochem*. 2019; 120:13751–64.
<https://doi.org/10.1002/jcb.28648>
PMID:[30957284](https://pubmed.ncbi.nlm.nih.gov/30957284/)
11. Pan C, Luo J, Zhang J. Computational Identification of RNA-Seq Based miRNA-Mediated Prognostic Modules in Cancer. *IEEE J Biomed Health Inform*. 2020; 24:626–33.
<https://doi.org/10.1109/JBHI.2019.2911528>
PMID:[30998483](https://pubmed.ncbi.nlm.nih.gov/30998483/)
12. Yin XH, Jin YH, Cao Y, Wong Y, Weng H, Sun C, Deng JH, Zeng XT. Development of a 21-miRNA Signature Associated With the Prognosis of Patients With Bladder Cancer. *Front Oncol*. 2019; 9:729.
<https://doi.org/10.3389/fonc.2019.00729>
PMID:[31448232](https://pubmed.ncbi.nlm.nih.gov/31448232/)
13. Liu CP, Zhang JH, Zheng SC, Liu J, Guo JC. A novel clinical multidimensional transcriptome signature predicts prognosis in bladder cancer. *Oncol Rep*. 2018; 40:2826–35.
<https://doi.org/10.3892/or.2018.6677>
PMID:[30226624](https://pubmed.ncbi.nlm.nih.gov/30226624/)
14. Pignot G, Cizeron-Clairac G, Vacher S, Susini A, Tozlu S, Vieillefond A, Zerbib M, Lidereau R, Debre B, Amsellem-Ouazana D, Bieche I. microRNA expression profile in a large series of bladder tumors: identification of a 3-miRNA signature associated with aggressiveness of muscle-invasive bladder cancer. *Int J Cancer*. 2013; 132:2479–91.
<https://doi.org/10.1002/ijc.27949>
PMID:[23169479](https://pubmed.ncbi.nlm.nih.gov/23169479/)
15. Tomczak K, Czerwińska P, Wiznerowicz M. The Cancer Genome Atlas (TCGA): an immeasurable source of knowledge. *Contemp Oncol (Pozn)*. 2015; 19:A68–77.
<https://doi.org/10.5114/wo.2014.47136>
PMID:[25691825](https://pubmed.ncbi.nlm.nih.gov/25691825/)
16. Ritchie ME, Phipson B, Wu D, Hu Y, Law CW, Shi W, Smyth GK. limma powers differential expression analyses for RNA-sequencing and microarray studies. *Nucleic Acids Res*. 2015; 43:e47.
<https://doi.org/10.1093/nar/gkv007>
PMID:[25605792](https://pubmed.ncbi.nlm.nih.gov/25605792/)

17. Yin H, He W, Li Y, Xu N, Zhu X, Lin Y, Gou X. Loss of DUSP2 predicts a poor prognosis in patients with bladder cancer. *Hum Pathol.* 2019; 85:152–61. <https://doi.org/10.1016/j.humpath.2018.11.007> PMID:30458195
18. Zhou H, Tang K, Xiao H, Zeng J, Guan W, Guo X, Xu H, Ye Z. A panel of eight-miRNA signature as a potential biomarker for predicting survival in bladder cancer. *J Exp Clin Cancer Res.* 2015; 34:53. <https://doi.org/10.1186/s13046-015-0167-0> PMID:25991007
19. Elango R, Alsaleh KA, Vishnubalaji R, Manikandan M, Ali AM, Abd El-Aziz N, Altheyab A, Al-Rikabi A, Alfayez M, Aldahmash A, Alajez NM. MicroRNA Expression Profiling on Paired Primary and Lymph Node Metastatic Breast Cancer Revealed Distinct microRNA Profile Associated With LNM. *Front Oncol.* 2020; 10:756. <https://doi.org/10.3389/fonc.2020.00756> PMID:32509578
20. Zhou XG, Huang XL, Liang SY, Tang SM, Wu SK, Huang TT, Mo ZN, Wang QY. Identifying miRNA and gene modules of colon cancer associated with pathological stage by weighted gene co-expression network analysis. *Onco Targets Ther.* 2018; 11:2815–30. <https://doi.org/10.2147/OTT.S163891> PMID:29844680
21. Meng X, Liu K, Xiang Z, Yu X, Wang P, Ma Q. MiR-125b-2-3p associates with prognosis of ccRCC through promoting tumor metastasis via targeting EGR1. *Am J Transl Res.* 2020; 12:5575–85. PMID:33042439
22. Zeng ZL, Lu JH, Wang Y, Sheng H, Wang YN, Chen ZH, Wu QN, Zheng JB, Chen YX, Yang DD, Yu K, Mo HY, Hu JJ, et al. The lncRNA XIST/miR-125b-2-3p axis modulates cell proliferation and chemotherapeutic sensitivity via targeting Wee1 in colorectal cancer. *Cancer Med.* 2021; 10:2423–41. <https://doi.org/10.1002/cam4.3777> PMID:33666372
23. Zheng ZN, Huang GZ, Wu QQ, Ye HY, Zeng WS, Lv XZ. NF-κB-mediated lncRNA AC007271.3 promotes carcinogenesis of oral squamous cell carcinoma by regulating miR-125b-2-3p/Slug. *Cell Death Dis.* 2020; 11:1055. <https://doi.org/10.1038/s41419-020-03257-4> PMID:33311454
24. Zheng ZQ, Li ZX, Zhou GQ, Lin L, Zhang LL, Lv JW, Huang XD, Liu RQ, Chen F, He XJ, Kou J, Zhang J, Wen X, et al. Long Noncoding RNA FAM225A Promotes Nasopharyngeal Carcinoma Tumorigenesis and Metastasis by Acting as ceRNA to Sponge miR-590-3p/miR-1275 and Upregulate ITGB3. *Cancer Res.* 2019; 79:4612–26. <https://doi.org/10.1158/0008-5472.CAN-19-0799> PMID:31331909
25. Salem M, Shan Y, Bernaudo S, Peng C. miR-590-3p Targets Cyclin G2 and FOXO3 to Promote Ovarian Cancer Cell Proliferation, Invasion, and Spheroid Formation. *Int J Mol Sci.* 2019; 20:1810. <https://doi.org/10.3390/ijms20081810> PMID:31013711
26. Yan M, Ye L, Feng X, Shi R, Sun Z, Li Z, Liu T. MicroRNA-590-3p inhibits invasion and metastasis in triple-negative breast cancer by targeting Slug. *Am J Cancer Res.* 2020; 10:965–74. PMID:32266103
27. Ji D, Qiao M, Yao Y, Li M, Chen H, Dong Q, Jia J, Cui X, Li Z, Xia J, Gu J. Serum-based microRNA signature predicts relapse and therapeutic outcome of adjuvant chemotherapy in colorectal cancer patients. *EBioMedicine.* 2018; 35:189–97. <https://doi.org/10.1016/j.ebiom.2018.08.042> PMID:30166271
28. Spagnuolo M, Costantini M, Ferriero M, Varmi M, Sperduti I, Regazzo G, Cicchillitti L, Díaz Méndez AB, Cigliana G, Pompeo V, Russo A, Laquintana V, Mastroianni R, et al. Urinary expression of let-7c cluster as non-invasive tool to assess the risk of disease progression in patients with high grade non-muscle invasive bladder Cancer: a pilot study. *J Exp Clin Cancer Res.* 2020; 39:68. <https://doi.org/10.1186/s13046-020-01550-w> PMID:32303246
29. Deng G, Wang R, Sun Y, Huang CP, Yeh S, You B, Feng C, Li G, Ma S, Chang C. Targeting androgen receptor (AR) with antiandrogen Enzalutamide increases prostate cancer cell invasion yet decreases bladder cancer cell invasion via differentially altering the AR/circRNA-ARC1/miR-125b-2-3p or miR-4736/PPARγ/MMP-9 signals. *Cell Death Differ.* 2021; 28:2145–59. <https://doi.org/10.1038/s41418-021-00743-w> PMID:34127806
30. Fan Y, Zhang L, Sun Y, Yang M, Wang X, Wu X, Huang W, Chen L, Pan S, Guan J. Expression profile and bioinformatics analysis of COMM10 in BALB/C mice and human. *Cancer Gene Ther.* 2020; 27:216–25. <https://doi.org/10.1038/s41417-019-0087-9> PMID:30787448
31. Zhu QL, Zhan DM, Chong YK, Ding L, Yang YG. MiR-652-3p promotes bladder cancer migration and invasion by targeting KCNN3. *Eur Rev Med Pharmacol Sci.* 2019; 23:8806–12. https://doi.org/10.26355/eurrev_201910_19275 PMID:31696467

32. Fredsøe J, Rasmussen AKI, Mouritzen P, Borre M, Ørntoft T, Sørensen KD. A five-microRNA model (pCaP) for predicting prostate cancer aggressiveness using cell-free urine. *Int J Cancer*. 2019; 145:2558–67. <https://doi.org/10.1002/ijc.32296>
PMID:[30903800](https://pubmed.ncbi.nlm.nih.gov/30903800/)
33. Xue X, Wang C, Xue Z, Wen J, Han J, Ma X, Zang X, Deng H, Guo R, Asuquo IP, Qin C, Wang H, Gao Q, et al. Exosomal miRNA profiling before and after surgery revealed potential diagnostic and prognostic markers for lung adenocarcinoma. *Acta Biochim Biophys Sin (Shanghai)*. 2020; 52:281–93. <https://doi.org/10.1093/abbs/gmz164>
PMID:[32073597](https://pubmed.ncbi.nlm.nih.gov/32073597/)
34. Zhang J, Gao S, Zhang Y, Yi H, Xu M, Xu J, Liu H, Ding Z, He H, Wang H, Hao Z, Sun L, Liu Y, Wei F. MiR-216a-5p inhibits tumorigenesis in Pancreatic Cancer by targeting TPT1/mTORC1 and is mediated by LINC01133. *Int J Biol Sci*. 2020; 16:2612–27. <https://doi.org/10.7150/ijbs.46822>
PMID:[32792860](https://pubmed.ncbi.nlm.nih.gov/32792860/)
35. Zhang Y, Lin P, Zou JY, Zou G, Wang WZ, Liu YL, Zhao HW, Fang AP. MiR-216a-5p act as a tumor suppressor, regulating the cell proliferation and metastasis by targeting PAK2 in breast cancer. *Eur Rev Med Pharmacol Sci*. 2019; 23:2469–75. https://doi.org/10.26355/eurrev_201903_17394
PMID:[30964173](https://pubmed.ncbi.nlm.nih.gov/30964173/)
36. Zhang Z, Zhang L, Wang B, Wei R, Wang Y, Wan J, Zhang C, Zhao L, Zhu X, Zhang Y, Chu C, Guo Q, Yin X, Li X. MiR-337-3p suppresses proliferation of epithelial ovarian cancer by targeting PIK3CA and PIK3CB. *Cancer Lett*. 2020; 469:54–67. <https://doi.org/10.1016/j.canlet.2019.10.021>
PMID:[31629932](https://pubmed.ncbi.nlm.nih.gov/31629932/)
37. Cao XM. Role of miR-337-3p and its target Rap1A in modulating proliferation, invasion, migration and apoptosis of cervical cancer cells. *Cancer Biomark*. 2019; 24:257–67. <https://doi.org/10.3233/CBM-181225>
PMID:[30883336](https://pubmed.ncbi.nlm.nih.gov/30883336/)

SUPPLEMENTARY MATERIALS

Supplementary Tables

Please browse Full Text version to see the data of Supplementary Table 1.

Supplementary Table 1. Downregulated miRNAs.

Supplementary Table 2. Multivariate Cox regression analysis of the 7 candidate miRNAs.

ID	coef	HR	HR.95L	HR.95H	<i>p</i> -value
hsa-let-7c-5p	-0.476175	0.621155	0.464975	0.829793	0.00127
hsa-miR-590-3p	-0.348215	0.705947	0.580388	0.85867	0.000492
hsa-miR-151a-5p	-0.210616	0.810085	0.644008	1.018989	0.071977
hsa-miR-337-3p	0.1619093	1.175754	1.006487	1.373487	0.041202
hsa-miR-125b-2-3p	0.3912236	1.478789	1.139598	1.918938	0.003251
hsa-miR-652-3p	-0.237091	0.788919	0.616345	1.009813	0.059778
hsa-miR-216a-5p	0.1524685	1.164706	1.038267	1.306541	0.00931